Annals of Nuclear Medicine Vol. 15, No. 6, 505–512, 2001

The role of whole-body FDG-PET in preoperative assessment of tumor staging in oral cancers

Yoshiki NAKASONE,* Tomio INOUE,** Noboru ORIUCHI,** Kazuo TAKEUCHI,***
Akihide NEGISHI,* Keigo ENDO** and Kenji MOGI*

*Departments of *Oral and Maxillofacial Surgery and **Nuclear Medicine, Gunma University, Faculty of Medicine*
****Takasaki University of Health and Welfare*

Objective: The aim of this study is to clarify the clinical utility of 2-deoxy-2-[^{18}F]fluoro-D-glucose (FDG) positron emission tomography (PET) in determining the TNM classification in patients with oral cancer. ***Methods:*** Twenty-five consecutive patients (14 male and 11 female; age range, 40 yr to 86 yr) with oral cancer were included in this study. The diagnostic accuracy for detecting cervical lymph nodes was investigated by comparing the results of CT and/or MRI and physical findings. For the semi-quantitative analysis, the tumor standardized uptake value (SUV) and tumor to background SUV ratio (T/B ratio) were assessed in primary tumors and cervical lymph nodes. ***Results:*** All primary lesions were visualized on FDG-PET images. Even though artifacts from dental materials near the lesion hampered the delineation of primary tumors on CT/MRI, the extent of primary tumors was accurately assessed by FDG-PET. The SUV and T/B ratio in the primary tumor classified in higher T grade (T3 and T4) was significantly higher than that in lower T grade (T1 and T2) (mean ± SD of SUV; 8.32 ± 2.99 vs. 5.15 ± 3.77, $p < 0.01$, mean ± SD of T/B ratio; 6.96 ± 3.23 vs. 3.61 ± 2.76, $p < 0.01$). The SUV and T/B ratio of metastatic lymph nodes were also significantly higher than those of normal lymph nodes (mean ± SD of SUV; 3.39 ± 1.69 vs. 1.55 ± 0.57, $p < 0.001$, mean ± SD of T/B ratio; 2.46 ± 1.08 vs. 1.03 ± 0.22, $p < 0.001$). Among these three methods, FDG-PET in conjunction with CT/MRI showed the highest accuracy of 92%, but there were no significant differences in diagnostic accuracy among the three methods. For the semi-quantitative analysis, a threshold SUV of 2.0 provided 100% sensitivity, 82% specificity, and 88% accuracy. Furthermore, a threshold T/B ratio of 1.5 provided 100% sensitivity, 100% specificity, and 100% accuracy. Regarding the detection of distant metastasis, there was one positive result in FDG-PET showing distant pulmonary metastasis. ***Conclusions:*** Whole-body FDG-PET is an effective and convenient diagnostic tool for the evaluation of tumor staging in patients with oral cancer. Tumor staging by whole-body FDG-PET may, in fact, supplement the conventional staging by means of CT/MRI and physical findings.

Key words: oral cancer, FDG-PET, SUV, cervical lymph node metastasis

INTRODUCTION

THE INCIDENCE of oral cancer is so high that more than 500,000 new patients are treated annually in the world.[1]

Oral cancer is, generally, a curable malignant tumor, since it can be detected at an early stage by simple inspection and palpation. The relatively long survival rate of the oral cancer patient requires maintenance of the patient's quality of life. From this viewpoint, the accurate assessment of the tumor extent based on the TNM classification is extremely important, but it is difficult to detect both the condition and the destruction of adjacent deep structures by tumor cell invasion. Likewise, it is also difficult to assess the presence of cervical lymph node metastases of oral cancer in a "clinically negative neck."

Received June 13, 2001, revision accepted September 13, 2001.

For reprint contact: Yoshiki Nakasone, M.D., Department of Oral and Maxillofacial Surgery, Gunma University, Faculty of Medicine, 3–39–22, Showa-machi, Maebashi, Gunma 371–8511, JAPAN.

E-mail: nakasone@med.gunma-u.ac.jp

Recent development of imaging methods such as CT and MRI has improved the diagnostic accuracy of TNM classification, but it is still limited, especially in detecting cervical lymph node metastasis.[2,3] Positron emission tomography (PET) with 2-deoxy-2-[^{18}F]fluoro-D-glucose (FDG) is now widely used in detecting head and neck cancer.[4,5] FDG-PET was proven to be useful in detecting cervical lymph node metastasis in patients with head and neck cancer, including various kinds of cancer such as laryngeal cancer and hypopharyngeal cancer,[6–8] but a few reports demonstrated the clinical utility of FDG-PET limited to oral cancer.[9] The aim of this study is to clarify the clinical utility of FDG-PET in determining the TNM classification in patients with oral cancers.

MATERIALS AND METHODS

Patients

Twenty-five consecutive patients (14 male and 11 female; age range, 40–86 yr) with oral cancers who underwent FDG-PET were included in this study. The clinical staging was based on the International Union Against Cancer (UICC, 1987) TNM-classification.[10] All patients had oral cancer. Pathological diagnoses of the primary lesions were established in all of them by biopsy and/or surgical specimen: 22 had squamous cell carcinoma, 2 basal cell carcinomas, and 1 verrucous carcinoma. In the group with squamous cell carcinoma, 10 patients had moderately differentiated types, and the remaining 12 patients had well-differentiated types. All positive results of cervical lymph node metastases in 8 patients were based on pathological diagnosis of surgical specimens. All negative results for cervical lymph nodes metastases were based on the clinical follow-up, including CT and/or MRI observation for more than one year. All patients underwent FDG-PET, CT and/or MRI before the treatments. There were no patients with diabetes mellitus in this study. Blood sugar levels in 24 patients were less than 100 mg/d*l* at the time of FDG injection. The blood sugar level in 1 patient (case 1) was 125 mg/d*l*. The patients and their tumor characteristics with the first physical findings are summarized in Table 1.

Table 1 Patients and tumor characteristics

Patient No.	sex/age (y)	Primary tumor		
		Location	Histological grade	TNM stage
1	M/55	tongue	M	T1N0M0
2	M/73	mandible	W	T1N0M0
3	M/77	mandible	M	T2N0M0
4	F/82	maxilla	M	T2N0M0
5	F/86	maxilla	M	T2N0M0
6	F/74	tongue	M	T2N0M0
7	M/65	tongue	M	T2N0M0
8	F/77	baccal mucosa	V	T2N0M0
9	F/64	maxilla	W	T2N0M0
10	F/70	maxilla	W	T2N0M0
11	M/48	maxilla	M	T2N1M0
12	M/49	maxilla	W	T2N1M0
13	M/45	tongue	W	T2N1M0
14	M/59	oral floor	M	T2N2M0
15	M/71	maxilla	W	T3N0M0
16	F/70	mandible	W	T3N1M0
17	M/46	tongue	W	T3N1M0
18	F/63	mandible	B	T4N0M0
19	F/77	maxilla	B	T4N0M0
20	F/40	mandible	M	T4N0M0
21	F/75	buccal mucosa	W	T4N0M0
22	M/78	maxilla	W	T4N1M0
23	M/65	mandible	M	T4N2M0
24	M/50	mandible	W	T4N2M0
25	M/66	mandible	W	T4N2M1*

B = Basal cell carcinoma, V = Verrucous carcinoma
M = moderately differentiated squamous cell carcinoma
W = well differentiated squamous cell carcinoma
*: lung metastasis was discovered with FDG-PET

PET studies

^{18}F was produced in an in-house cyclotron BC1710 (Japan Steel Works, Muroran, Japan), and FDG was synthesized by the Hamacher method.[11] PET images were obtained with a SET 2400W (Shimadzu Corporation, Kyoto, Japan) with a 59.5-cm transaxial field of view, 20-cm axial field of view, which produced 63 image planes, spaced 3.125 mm apart. Transaxial spatial resolution was 4.2 mm full width at half maximum (FWHM) at the center of the field of view and axial resolution was 5.0 mm FWHM. In the case of FDG-PET, a whole body image obtained by the simultaneous emission-transmission method with a rotating external source[12] was started at 60 min after the injection of 5 MBq/kg (body weight) by the multiple-bed position technique. Four to five sections from head to thigh were imaged for 8 min per section. Patients fasted at least 4 hours before FDG injection. The imaging protocols of FDG-PET were approved by the Institutional Review Board of our institute, and all the patients gave informed consent to undergo the above examination.

Attenuation-corrected transaxial images with FDG were reconstructed by the ordered subsets expectation maximization (OS-EM) algorithm into 128 × 128 matrices with pixel dimensions of 4.0 mm in a plane and 3.125 mm axially. Finally, 3 consecutive slices were added to generate a transaxial image slice 9.8 mm thick for visual interpretation and quantitative analysis by using the standardized uptake value (SUV). Coronal image slices 9.8 mm thick were also reconstructed from attenuation-corrected transaxial images.

CT/MRI

Twenty-four patients were examined by CT with the patient in the supine position. CT was performed with a Hi-speed helical CT scanner and LightSpeed QX/i scan-

ner (GE Medical Systems, Milwaukee, Wis, USA). Plain axial CT images of 5 mm thick slices were provided from the infraorbital plane to the hyoid bone. After bolus administration of contrast material, 5 mm thick slice images were scanned from the infraorbital plane to the supraclavicular region including whole cervical lymph nodes around the sternocleidomastoid muscle.

Thirteen patients were examined with MRI by using a head coil and a neck coil with the patient in the supine position. MRI was performed with 1.5 T SIGNA Horizon LX (GE Medical Systems, Milwaukee, Wis, USA) and 1.5 T MAGNETOM Symphony (Siemens Medical Systems, Erlangen, Germany). Transaxial T1-weighted (500–600/10–15 [repetition time msec/echo time msec]) and T2-weighted (3000–5000/90–100) spin-echo imagings were obtained before the administration of contrast material. After the first examination, contrast-enhanced T1-weighted images were obtained. Fat saturation was added to T2-weighted images and T1-weighted images after the administration of 0.2 m*l*/kg of gadodiamido hydrate (Omniscan, Daiichi Seiyaku) in the case of invasion of adjacent fat tissue.

Radiologic criteria referring to the description of cervical lymph node metastasis[13,14] were used as follows.

1. Nodes with a minimal diameter of 10 mm or more in all cervical and submandibular regions were considered to have a high probability of metastasis.
2. Nodes with irregular enhancement and ring-like enhancement were considered to have a high probability of metastasis.
3. Nodes with an irregular or rough rim were considered to have a high probability of metastasis.
4. Nodes with identified extranodal spread on the images were considered to have a high probability of metastasis.

Data analysis

Transaxial and coronal FDG-PET images were prospectively interpreted visually by two nuclear radiologists in conjunction with CT or MRI until a consensus was reached.

Compared with the surrounding background radioactivity, uptake scores of lesions were defined as no uptake (−), faint uptake (+/−), moderate uptake (+), and definitely abnormal intense uptake (++). No uptake area was defined as a photo deficient area. Faint uptake meant almost the same radioactivity as background activity. Definitely abnormal intense uptake was defined to be closed brain FDG uptake. Moderate uptake was between faint uptake and definitely abnormal intense uptake. Moderate uptake (+) and definitely abnormal intense uptake (++) were defined as positive results for detecting malignant tumors, and no uptake (−) and faint uptake (+/−) were defined as negative results. All PET results of visual interpretation were finally compared with the standard conventional images such as CT, MRI, and results of pathological diagnosis. From attenuation-corrected transaxial images, the injected dose of FDG, body weight and cross calibration factors between PET and the dose calibrator, functional images of standardized uptake value (SUV) were also generated.

SUV was defined as follows;

$$\text{SUV} = \frac{\text{Radioactive concentration in tissue or lesion (MBq/g)}}{\text{Injected dose (MBq)/patient's body weight (g)}}$$

Regions of interest (ROIs) 1 cm in diameter, including the maximum value, were drawn on areas corresponding to lesions larger than 2 cm in diameter. If the lesion was less than 2 cm in diameter, ROI was drawn over the entire lesion but the partial volume effect was not corrected. Regarding non-visualized regional lymph nodes on PET images, ROIs 1 cm in diameter were drawn on the corresponding area with the fusion image combined with CT images.[15] A background ROI of the same diameter as that of the ROI defined on the primary lesion was drawn over the corresponding area in the opposite site. If the primary lesion was located near the center of the oral cavity, background ROI was defined the surrounding background area. The average value per pixel in the ROI was employed for assessing SUV of the primary lesion. Regarding the cervical lymph node, the maximum value per pixel in the ROI was computed for assessing the SUV of both the lesion in the lymph node for the target and normal lymph node for the background. The SUVs of lesions and the target-to-background SUV ratios (T/B ratios) were derived from a FDG-PET study. Data were divided into three categories: primary tumor lesion (T), cervical lymph nodes (N) and distant metastasis (M).

Regarding the analysis of PET results for primary tumors, we investigated the relationships between FDG uptake and the T grade in TNM classification by UICC, the existence of regional cervical lymph node metastasis, and histological differentiation. They were also analyzed for diagnostic ability related to sensitivity, specificity, positive predictive value (PPV) and negative predictive value (NPV) among CT/MRI, physical findings, and FDG-PET.

Statistical analysis

Differences in the primary tumor SUV and T/B ratio among T grades in the TNM classification were statistically estimated by non-parametric Mann-Whitney test. Differences in the primary tumor SUV and T/B ratio among tumor gradings of Broders' classification, and those between the group with lymph node metastasis and that without lymph node metastasis were also evaluated by non-parametric Mann-Whitney test.

Differences in sensitivity and specificity were statistically evaluated by non-parametric McNemar's test and differences in the PPV and NPV were statistically analyzed by the method proposed by Leisenring et al.[16] In all

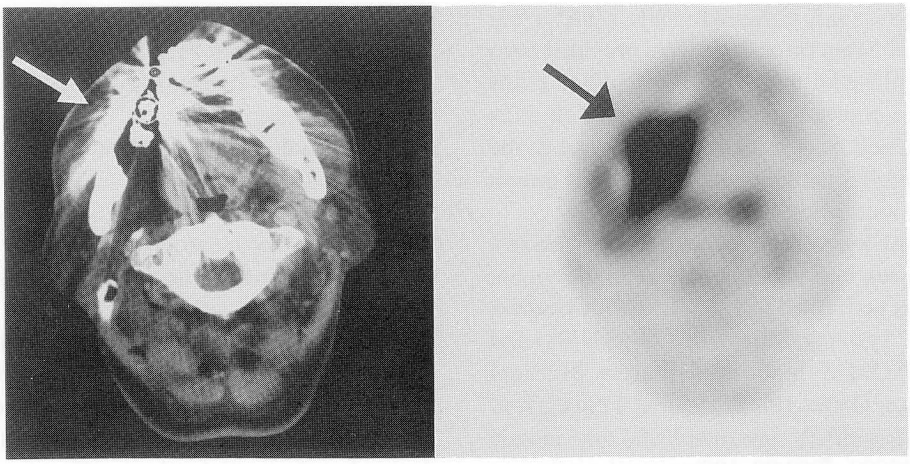

Fig. 1 Case 23. (A) Axial CT demonstrates artifacts from dental materials near the lesion hampered the detection of primary tumor (arrow). (B) FDG-PET detected high accumulation (SUV = 7.57, T/B = 8.60) in the right mandible (arrow).

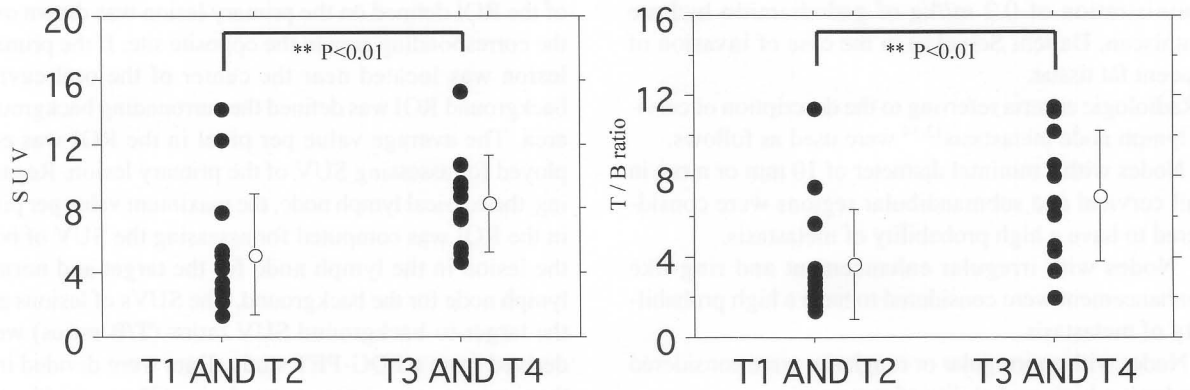

Fig. 2 FDG uptake and T grades of primary tumors. (left) Regarding T grade in TNM classification by UICC, the SUV in the lower T grade (T1 and T2) cancer ranged from 1.36 to 14.10 with a mean ± S.D. of 5.15 ± 3.77 (n = 14) and in higher T grade (T3 and T4) cancer ranged from 4.79 to 15.34 with a mean ± S.D. of 8.32 ± 2.99 (n = 11). (right) The T/B ratio in the lower T grade (T1 and T2) cancer ranged from 1.35 to 11.28 with a mean ± S.D. of 3.61 ± 2.76 (n = 14) and in higher T grade (T3 and T4) cancer ranged from 1.98 to 11.47 with a mean ± S.D. of 6.96 ± 3.23 (n = 11). Open circle and vertical bars represent mean ± S.D.

statistical analyses of this study, a p value less than 0.05 was defined as significant.

RESULTS

All primary lesions were visualized on FDG-PET images. Even though artifacts from dental materials near the lesion hampered the detection of primary tumors on CT/MRI in cases 15, 20 and 23, the extent of primary tumors was accurately assessed by FDG-PET in conjunction with CT/MRI (Fig. 1).

Regarding the T grade, FDG uptake of SUV and the T/B ratio in the primary tumor classified in higher T grades (T3 and T4) was significantly higher than that in lower T grades (T1 and T2) (Fig. 2), but there were overlaps between the FDG uptakes in lower T grades and those in higher T grades. With respect to the existence of cervical lymph node metastasis, there were also no significant differences between FDG uptake by the primary tumor in patients with cervical lymph node metastasis and that in patients without cervical lymph node metastasis. There were no significant differences in SUV and the T/B ratio among tumor differentiation.

Regarding cervical lymph node metastasis, the first physical findings showed metastatic lymph nodes in 10 patients, but pathological findings proved true lymph node metastasis in 8 patients. Concerning the analysis of FDG-PET results in detecting cervical lymph node metastasis, comparative studies of FDG-PET, CT/MRI and physical findings were conducted prospectively. Among the three methods, FDG-PET in conjunction with CT/MRI showed the highest accuracy of 92% and had 88%

Table 2 Diagnostic accuracy for detecting cervical lymph nodes metastases

	Sensitivity (%)	Specificity (%)	PPV	NPV
FDG-PET in conjunction with CT/MRI	88 (7/8)*	94 (16/17)*	88 (7/8)*	94 (16/17)*
CT/MRI alone	63 (5/8)	88 (15/17)	71 (5/7)	83 (15/18)
Physical alone	88 (7/8)	82 (14/17)	70 (7/10)	93 (14/15)

PPV = positive predictive value. NPV = negative predictive value
* not significantly different from CT/MRI and physical findings

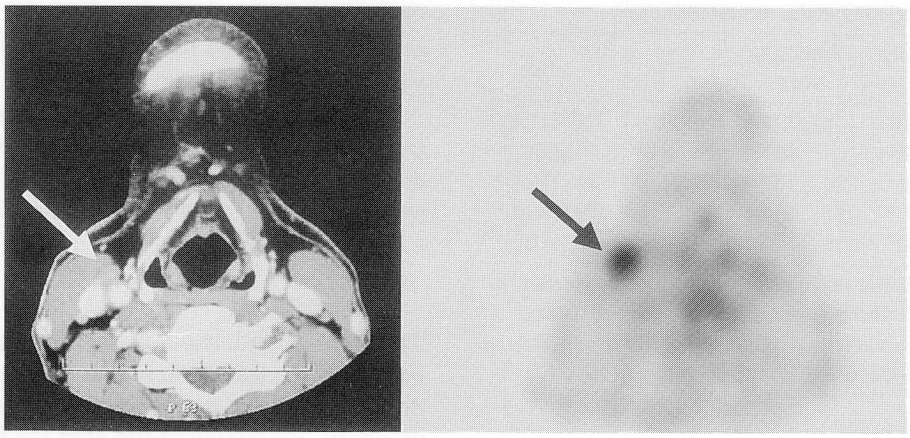

Fig. 3 Case 17. (A) Axial CT with contrast enhancement showed right cervical lymph node in diameter less than 10 mm (arrow). (B) FDG-PET through the same level as A. The accumulation of cervical lymph node (SUV= 3.37, T/B = 2.15) was shown (arrow). Histopathologically, this lymph node was proven to be metastasis of squamous cell carcinoma in the right tongue.

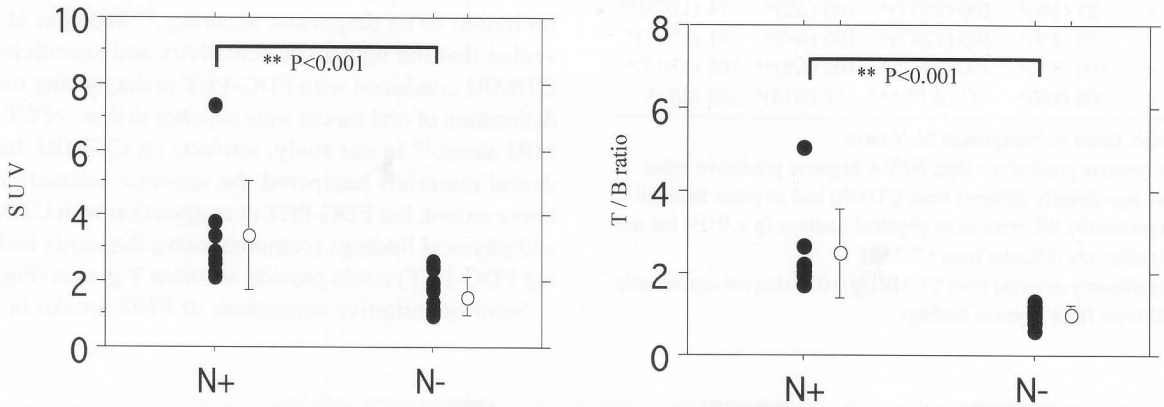

Fig. 4 FDG uptake of cervical lymph nodes. (left) The SUV of metastatic lymph node ranged from 2.13 to 7.35 with a mean ± S.D. of 3.39 ± 1.69 (n = 8) and that of normal lymph node ranged from 8.95 to 2.64 with a mean ± S.D. of 1.55 ± 0.57 (n = 17). (right) The T/B ratios of metastatic lymph node ranged from 1.63 to 5.03 with a mean ± S.D. of 2.46 ± 1.08 (n = 8) and that of normal lymph node ranged from 0.61 to 1.49 with a mean ± S.D. of 1.03 ± 0.22 (n = 17). Open circle and vertical bars represent mean ± S.D.

sensitivity (7/8), 94% specificity (16/17), 88% PPV (7/8), and 94% NPV (16/17). The diagnostic accuracy of FDG-PET in conjunction with CT/MRI was shown to be the most effective means of detecting cervical lymph node metastasis (Table 2). There were one false positive result and one false negative result of FDG-PET found by visual interpretation in detecting cervical lymph node metastasis. The false positive result has well-differentiated SCC in the median maxilla, and there was shown to be moderate uptake in the right upper cervical lymph node. On the other hand, the false negative result has also well-differentiated SCC in the right maxilla, and there was shown to be faint uptake in the right upper cervical lymph node. There were two false negative results of CT/MRI in detecting cervical lymph node metastasis. Both cases showed true positive results in FDG-PET and in physical

findings (cases 13 and 17) (Fig. 3). There were two false positive results in CT/MR imaging (cases 18 and 25). In both cases FDG-PET showed true negative results and in case 18 physical findings also showed a true negative result. In physical findings, three cases (cases 16, 22 and 25) showed false positive results in detecting cervical lymph node metastasis. In case 16, both FDG-PET and CT/MRI showed true negative results. For the semi-quantitative analysis, both SUV and the T/B ratio of metastatic lymph nodes were significantly higher ($p < 0.001$) than those of normal lymph nodes (Fig. 4). In contrast to the results of visual interpretation in detecting cervical lymph node metastasis (sensitivity 88%, specificity 94% and accuracy 92%) (Table 2), a threshold SUV of 2.0 provided 100% sensitivity, 82% specificity and 88% accuracy (Table 3). Furthermore, a threshold T/B ratio of 1.5 provided 100% sensitivity, 100% specificity and 100% accuracy (Table 4).

As for the detection of distant metastasis, there was one positive result in FDG-PET (case 25) (Fig. 5) showing distant pulmonary metastasis, and the patient died as result of progression of the metastatic disease.

Table 3 SUV threshold and diagnostic accuracy for detecting cervical lymph nodes metastases

SUV Threshold	Sensitivity (%)	Specificity (%)	PPV	NPV
3.5 <	25 (2/8)*	100 (17/17)*	100 (2/2)*	74 (17/23)**
3.0 <	38 (3/8)*	100 (17/17)*	100 (3/3)*	77 (17/22)**
2.5 <	75 (6/8)*	88 (15/17)*	75 (6/8)*	88 (15/17)*
2.0 <	100 (8.8)*	82 (14/17)*	73 (8/11)*	100 (14/14)*
1.5 <	100 (8.8)*	59 (10/17)*	57 (8/14)*	100 (11/11)*

PPV = positive predictive value, NPV = negative predictive value
* not significantly different from CT/MRI and physical findings
** significantly different from physical findings ($p < 0.05$) but not significantly different from CT/MRI

Table 4 T/B ratio threshold and diagnostic accuracy for detecting cervical lymph nodes metastases

T/B ratio Threshold	Sensitivity (%)	Specificity (%)	PPV	NPV
2.5 <	25 (2/8)*	100 (17/17)*	100 (2/2)*	74 (17/23)**
2.0 <	50 (4/8)*	100 (17/17)*	100 (4/4)*	81 (17/21)*
1.5 <	100 (8/8)*	100 (17/17)*	100 (8/8)**	100 (17/17)*
1.0 <	100 (8/8)*	47 (8/17)***	57 (8/14)*	100 (8/8)*

T/B ratio: target-to-background SUV ratio
PPV = positive predictive value, NPV = negative predictive value
* not significantly different from CT/MRI and physical findings
** significantly different from physical findings ($p < 0.05$) but not significantly different from CT/MRI
*** significantly different from CT/MRI ($p < 0.05$) but not significantly different from physical findings

DISCUSSION

The TNM classification is widely accepted for treating patients with oral cancer because the optimal treatment depending on the tumor staging affects the patients, prognosis and quality of life after the first treatment.[17] The estimation by physical findings by an oral surgeon is essentially important, but such findings are empirical but not objective. The imaging examinations such as CT and MRI can provide objective, precise anatomical information on primary tumor invasion but there is still some limitation to its diagnostic accuracy.[18] Wong et al. revealed that the diagnostic sensitivity and specificity of CT/MRI combined with FDG-PET in diagnosing tumor delineation of oral cancer were superior to those of CT and MRI alone.[19] In our study, artifacts on CT/MRI due to dental materials hampered the accurate estimation of tumor extent, but FDG-PET in conjunction with CT/MRI and physical findings (comprehensive diagnosis including FDG-PET) could provide accurate T grades (Fig. 1).

Semi-quantitative estimation of FDG uptake in pri-

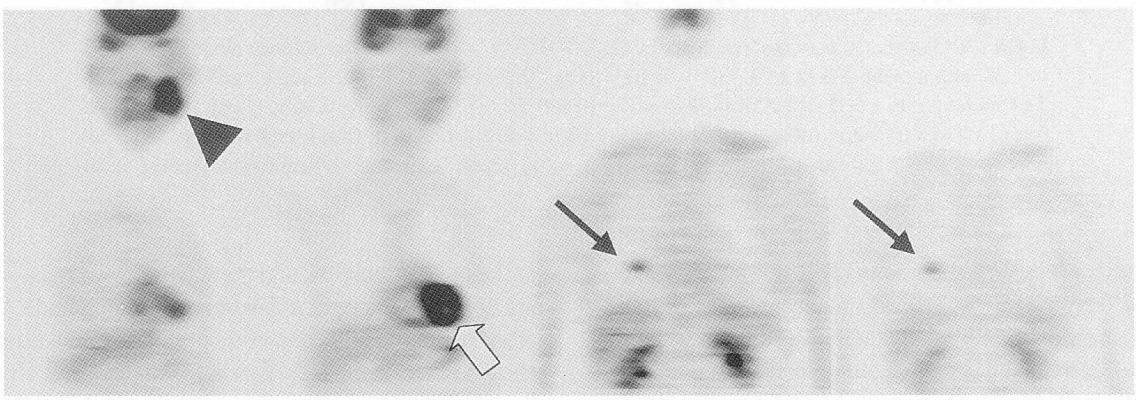

Fig. 5 Case 25. FDG-PET showed the distant metastasis in right lower lung (arrows). High FDG accumulation of the primary tumor was observed in the left mandible (SUV = 10.67, T/B = 11.47) (arrow head). The physiological uptake of FDG was shown in the heart (open arrow).

mary tumors did not provide any clinically useful information about initial tumor staging because there were overlaps of FDG uptake between lower T grades and higher T grades (Fig. 2). Generally T grades have been divided into 4 but in our study there was a distinction between lower and higher T grades. Because there were insufficient T grades to analyze statistically. And there was no significant difference between FDG uptake of primary tumors in patients with lymph node metastasis and in patients without lymph node metastasis.

Comprehensive FDG-PET can provide information on tumor metabolism related to tumor aggressiveness. There was no significant difference in FDG tumor uptake between well-differentiated squamous cell cancer (G1 in Broder's classification) and moderately differentiated squamous cell cancer (G2 in Broder's classification). Because there were no patients with tumor gradings of G3 or G4 in our series, the relationship between FDG tumor uptake and tumor grading of oral cancer should be investigated in a greater number of patients with G3 and G4 grades.

The 5-year overall survival in patients with oral cancer was reported to be 33.4%, and survival by TNM cancer stage was reported to be 64.6% in stage I, 67.5% in stage II, 28.9% in stage III and 13.1% in stage IV.[20] There seemed to be a significant difference between stages II and III. Because patients with cervical lymph node metastasis (N1) are categorized in stage III, accurate estimation of the N stage is clinically crucial. Regarding the detection of cervical lymph node metastasis from oral cancer, a number of articles reported that the diagnostic accuracy of FDG-PET was superior to that of CT/MRI alone or physical findings.[21,22] There were no significant statistical differences in our study. But sensitivity, specificity, PPV and NPV of FDG-PET based on the visual interpretation combined with CT/MRI were superior to those of CT/MRI and physical findings alone (Table 2). The N-staging estimation by conventional the method with physical findings and CT/MRI examination were accurately modified in 2 patients by adding the FDG-PET estimation (upgrading in no patient, downgrading in 2 patients). Two cases were misinterpreted visually. One case was interpreted as a cervical lymph node metastasis, but actually after following up for one year, the lymph nodes remained normal (case 22). Inflammatory change in cervical lymph nodes always troubled us by leading to a different diagnosis from tumor. Another case was shown to be faint uptake of FDG and visually diagnosed as negative for cervical lymph node metastasis, but metastatic lymph nodes were found in the right upper neck on pathological diagnosis (case 10). These two cases proved the difficulty of diagnosis in FDG-PET by visual interpretation only. The advantage of N-staging with FDG-PET was that objective data such as SUV and the T/B ratio could be obtained from the functional SUV images. An SUV threshold of 2 and a T/B ratio threshold of 1.5 yielded the most appropriate diagnostic accuracy of 100% in detecting cervical lymph node metastasis (Tables 3 and 4). Our study showed that using the T/B ratio in detecting cervical lymph node metastasis can be the most effective method of FDG-PET in conjunction with conventional CT/MRI and physical findings in such a limited number of cases. The partial volume averaging on SUV analysis in small lesions of regional lymph node metastasis was problematic in the accurate estimation of the N stage. In this study, the size of lesions in cervical lymph node metastasis ranged from 10 mm to 20 mm in diameter with a corresponding recovery coefficient of from 0.5 to 0.9 with our PET camera.[23] We tried to estimate the diagnostic accuracy of SUV analysis by using the partial volume correction formula derived from our fundamental experiment but failed to obtain good results because of the worsening of diagnostic specificity; in other words, because of the over-estimation of SUV in small lymph nodes without metastasis (data not presented). Therefore we assessed the maximum ROI value on cervical lymph node for the semi-quantitative analysis to avoid the partial volume effect.

Although N-staging in the UICC classification is not referred to in the localization of cervical lymph node metastasis, the procedure of surgical neck dissection largely depends on its localization. For example, supraomohyoid neck dissection should be conducted in patients with N0 and N1 of submandibular lymph node metastasis, and radical neck dissection should be selected in patients with lymph node metastasis beyond the submandibular lymph node. The identification of lymph node metastasis beyond submandibular lymph nodes could be accurately conducted by means of FDG-PET in addition to CT/MRI (Fig. 3). A new method with a combined PET/CT scanner is expected to detect the location more clearly.[24] The usefulness of FDG-PET combined with MRI/CT for the evaluation of extranodal spread was not assessed in this study because of the absence of patients with extranodal spread. Many reports have shown the high ability to detect cervical lymph node metastasis by FDG-PET.[2,3,9] Our study showed a more effective (100% accuracy) method for detecting cervical lymph node metastasis by using T/B ratio of the maximum value in each ROI, the average for the ROI was also used in detecting the primary tumor. However cervical lymph nodes were not large enough to be represented accurately by average for the ROI. Therefore we used the maximum value to avoid underestimation and to secure reproducibility.

Regarding the detection of distant metastasis, the whole-body FDG-PET was useful in a patient with lung metastasis (Fig. 5). In cases in the M1 stage, chemotherapy and/or radiation therapy should be selected as the first treatment for oral cancer.[25] Another clinical advantage of whole-body FDG-PET is to detect second primary cancer in patients with oral cancer.[26]

In conclusion, whole-body FDG-PET is an effective

and convenient diagnostic tool for the evaluation of tumor staging in patients with oral cancer. Tumor staging by whole-body FDG-PET may, in fact, supplement conventional staging with CT/MRI and physical findings, but further studies will produce more conclusive results.

REFERENCES

1. Vokes EE, Weichselbaum RR, Lippman SM, Hong WK. Head and neck cancer. *N Engl J Med* 1993; 328: 184–194.
2. Adams S, Baum RP, Stuckensen T, Bitter K, Hor G. Prospective comparison of ^{18}F-FDG PET with conventional imaging modalities (CT, MRI, US) in lymph node staging of head and neck cancer. *Eur J Nucl Med* 1998; 25: 1255–1260.
3. Benchaou M, Lehmann W, Slosman DO, Becker M, Lemoine R, Rufenacht D, et al. The role of FDG-PET in the preoperative assessment of N-staging in head and neck cancer. *Acta Otolaryngol* 1996; 116: 332–335.
4. Keyes JW Jr, Watson NE Jr, Williams DW 3rd, Greven KM, McGuirt WF. FDG PET in head and neck cancer. *AJR* 1997; 169: 1663–1669.
5. Jabour BA, Choi Y, Hoh CK, Rege SD, Soong JC, Lufkin RB, et al. Extracranial head and neck: PET imaging with 2-[F-18]fluoro-2-deoxy-D-glucose and MR imaging correlation. *Radiology* 1993; 186: 27–35.
6. AAssar OS, Fischbein NJ, Caputo GR, Kaplan MJ, Price DC, Singer MI, et al. Metastatic head and neck cancer: role and usefulness of FDG PET in locating occult primary tumors. *Radiology* 1999; 210: 177–181.
7. Stokkel MPM, Terhaad CH, Hordijk GJ, van Rijk PP. The detection of unknown primary tumors in patients with cervical metastases by dual-head positron emission tomography. *Oral Oncology* 1999; 35: 390–394.
8. Mukherji SK, Drane WE, Mancuso AA, Parsons JT, Mendenhall WM, Stringer S. Occult primary tumors of the head and neck: detection with 2-[F-18]fluoro-2-deoxy-D-glucose SPECT. *Radiology* 1996; 199: 761–766.
9. Stuckensen T, Kovacs AF, Adams S, Baum RP. Staging of the neck in patients with oral cavity squamous cell carcinomas: a prospective comparison of PET, ultrasound, CT and MRI. *J Maxillofac Surg* 2000; 28: 319–324.
10. UICC: *TNM Classification of Malignant Tumors. 4th ed*, Hermanek P, Sobin LH (eds), Berlin, Germany; Springer-Verlag, 1987.
11. Hamacher K, Coenen HH, Stocklin G. Efficient stereospecific synthesis of no-carrier-added 2-[^{18}F]-fluoro-2-deoxy-D-glucose using aminopolyether supported nucleophilic substitution. *J Nucl Med* 1986; 27: 235–238.
12. Inoue T, Oriuchi N, Kunio M, Tomiyoshi K, Tomaru Y, Aoyagi K, et al. Accuracy of standardized uptake value measured by simultaneous emission and transmission scanning in PET oncology. *Nucl Med Commun* 1999; 20: 849–857.
13. Don DM, Anzai Y, Lufkin RB, Fu YS, Calcaterra TC. Evaluation of cervical lymph node metastases in squamous cell carcinoma of the head and neck. *Laryngoscope* 1995; 105: 669–674.
14. van den Brekel MW, Stel HV, Castelijns JA, Nauta JJ, van den Waal I, Valk J, et al. Cervical lymph node metastasis: assessment of radiologic criteria. *Radiology* 1990; 177: 379–384.
15. Saleh A, Inoue T, Zhang H, Ahmed K, Oriuchi N, Sato N, et al. Image fusion system using PACS for MRI, CT, and PET images. *Clin Pos Imag* 1999; 2: 137–143.
16. Leisenring W, Alonzo T, Pepe MS. Comparisons of predictive values of binary medical diagnostic tests for paired designs. *Biometrics* 2000; 56: 345–351.
17. Rogers SN, Lowe D, Brown JS, Vaughan ED. The University of Washington head and neck cancer measure as a predictor of outcome following primary surgery for oral cancer. *Head Neck* 1999; 21: 394–401.
18. Wong WL, Chevretton EB, McGurk M, Hussain K, Davis J, Beaney R, et al. A prospective study of PET-FDG imaging for the assessment of head and neck squamous cell carcinoma. *Clin Otolaryngol* 1997; 22: 209–214.
19. Wong WL, Hussain K, Chevretton E, Hawkes DJ, Baddeley H, Maisey M, et al. Validation and clinical application of computer-combined computed tomography and positron emission tomography with 2-[^{18}F]fluoro-2-deoxy-D-glucose head and neck images. *Am J Surg* 1996; 172: 628–632.
20. Ribeiro KC, Kowalski LP, Latorre MR. Impact of comorbidity, symptoms, and patients' characteristics on the prognosis of oral carcinomas. *Arch Otolaryngol Head Neck Surg* 2000; 126: 1079–1085.
21. Stokkel MPM, ten Broek FW, van Rijk PP. Preoperative assessment of cervical lymph nodes in head and neck cancer with fluorine-18 fluorodeoxyglucose using a dual-head coincidence camera: a pilot study. *Eur J Nucl Med* 1999; 26: 499–503.
22. Myers LL, Wax MK. Positron emission tomography in the evaluation of the negative neck in patients with oral cavity cancer. *J Otolaryngol* 1998; 27: 342–347.
23. Zhang H, Inoue T, Alyafei S, Tian M, Oriuchi N, Ichikawa A, et al. Fundamental study of hot spot detectability in 3-dimensional positron emission tomography. *Ann Nucl Med* 2000; 14: 279–284.
24. Beyer T, Townsend DW, Brun T, Kinahan PE, Charron M, Roddy R, et al. A combined PET/CT scanner for clinical oncology. *J Nucl Med* 2000; 41: 1369–1379.
25. Alvi A, Johnson JT. Development of distant metastasis after treatment of advanced-stage head and neck cancer. *Head Neck* 1997; 19: 500–505.
26. Stokkel MP, Moons KG, ten Broek FW, van Rijk PP, Hordijk GJ. ^{18}F-fluorodeoxyglucose dual-head positron emission tomography as a procedure for detecting simultaneous primary tumors in cases of head and neck cancer. *Cancer* 1999; 86: 2370–2377.